Theor Chem Acc (1998) 100:212–221
DOI 10.1007/s002149800m57

Theoretical
Chemistry Accounts

Regular article

Ab initio quantum chemical study of the formation, decomposition and isomerization of the formaldiminoxy radical (CH_2NO): comparison of the Gaussian-2 and CASPT2 techniques in the calculation of potential energy surfaces*

Warwick A. Shapley, George B. Bacskay

School of Chemistry, University of Sydney, NSW 2006, Australia

Received: 8 May 1998 / Accepted: 11 August / Published online: 9 October 1998

Abstract. The reaction between triplet methylene and nitric oxide, producing the formaldiminoxy (CH_2NO) radical, and the subsequent decomposition and isomerization reactions of CH_2NO have been studied using ab initio quantum chemical techniques that include the Gaussian-2 (G2), CASSCF and CASPT2 methods. Stationary points on the potential energy surfaces were located at MP2/6-31G(*d*) and CASSCF/cc-pVDZ levels of theory, while the electronic energies were determined using G2, G2(MP2), QCISD(T)/cc-pVTZ, RCCSD(T)/cc-pVTZ and CASPT2/cc-pVTZ approaches. G2 is believed to be reliable at equilibrium geometries, but the determination of certain transition state geometries and energies requires a MCSCF-based approach. The calculations suggest that CH_2NO ($^2A'$) forms in a barrierless reaction and could readily decompose to $H + HCNO$. A subsequent abstraction reaction then results in $H_2 + CNO$. No molecular elimination channel was found. An alternative pathway is the formation of CH_2ON, which readily isomerizes to CH_2NO.

Key words: Combustion reactions – Potential energy surfaces – CASPT2 – Gaussian-2

1 Introduction

Nitric oxide (NO) has long been recognized as one of the major by-products formed during the combustion of fuels and many studies have been undertaken with a view to learning how to control the production of this atmospheric pollutant [1]. One of the ways in which NO is formed is via the "prompt NO" mechanism [2], whereby small hydrocarbon radicals such as C, CH, CH_2 and CH_3 react with atmospheric nitrogen at the high temperatures prevalent in such systems (typically between 500 K and 2500 K) and thus initiate a series of reactions resulting in the production of NO. Conversely, the amount of NO produced during combustion may be reduced through reaction of NO with these same hydrocarbon radicals, a process referred to as "reburning" [3–6]. It is desirable, therefore, to have accurate data on the mechanisms, rates and energetics of the elementary reactions governing such NO_x producing and reducing processes, which may then be used in the modelling of combustion systems.

With regard to methylene, a number of experiments have been performed that directly measure the rate constant for the reaction

$$CH_2 + NO \rightarrow \text{products} \quad (1)$$

in the gas phase [7–10]. In addition, formation and detection of the formaldiminoxy molecule (CH_2NO) has been achieved in the gas phase [10] by reaction (1), by photodissociation of the nitromethyl radical [11] (CH_2NO_2) and by photolysis (in an argon matrix at low temperatures) of diazomethane [12] (CH_2N_2) or of ketene [13] (CH_2CO) in the presence of NO. The acquisition of kinetic data is, however, hampered by the fact that most intermediate species in these reactions are radicals with very short lifetimes and therefore difficult to detect experimentally.

Such problems are, of course, not encountered in theoretical studies of the problem and in fact such studies, utilizing quantum chemical methods, have the potential to provide accurate thermodynamic and rate parameters for the successful kinetic modelling of the above reactions. In order to obtain meaningful results, however, reasonably high levels of theory must be used, so as to provide heats of reactions and critical energies of near chemical accuracy (about ± 2 kcal/mol).

* Dedicated to Prof. Dr. Wilfried Meyer on the occasion of his 60th birthday

Correspondence to: G.B. Bacskay

Whilst reasonably accurate equilibrium geometries can be obtained using a relatively low level of theory, such as Hartree-Fock (HF) or second-order Møller-Plesset perturbation theory (MP2), with basis sets of double-zeta plus polarization functions quality, transition state geometries, particularly those corresponding to bond breaking and forming reactions, often exhibit near-degeneracy effects that may well necessitate the use of multiconfigurational SCF (MCSCF) [14–17] wave functions or an approach that is based on a multireference expansion of the wave function. The calculation of chemically accurate energies of course requires accurate treatment of electron correlation, i.e. high levels of theory applied in conjunction with extended basis sets. The Gaussian theories G1 [18, 19], G2 [20] and G2(MP2) [21] developed by Pople and coworkers, specifically formulated with the reliable computation of thermochemistry in mind, are based on single-reference descriptions of molecules. In particular, the equilibrium geometries are obtained by the MP2 method, while the energy is calculated by the quadratic configuration interaction (QCI) method [22] in conjunction with a modest basis set, viz. 6-311G(*d*,*p*). The latter is corrected for basis truncation effects via a series of lower level (MP2, MP4) calculations with successively larger basis sets. The G2 and G2(MP2) methods have proved to be remarkably accurate in the calculation of thermochemical data, such as heats of atomization, where an accuracy of ~1 kcal/mol has been achieved in the introductory study on 55 molecules (composed of first-row atoms). As a result, G2 has become a useful benchmark with which the predictions of other approaches are often compared.

In situations where single reference based techniques may be inaccurate or even inappropriate, such as transition states, multireference approaches must be used such as the complete active space SCF (CASSCF), multireference CI (MRCI) [23] or CASPT2 [24, 25], where a CASSCF wave function is the reference state in a second-order perturbation calculation of the dynamic correlation contributions to the energy not resolved at the CASSCF level. Given the low cost of CASPT2 (in comparison with MRCI), it is a particularly attractive method as it has "universal" applicability and is capable of describing equilibrium and transition state structures equally well. Recent work, mostly by Andersson and coworkers [26, 27], has demonstrated the capability and accuracy of CASPT2 in a number of interesting applications.

In this, the first of a series of papers that aims to comprehensively characterize the CH_2NO and HCNO systems, we report the results of our calculations on the radical-radical reaction

$$CH_2(^3B_1) + NO(^2\Pi) \rightarrow CH_2NO(^2A', ^2A'') \quad (2)$$

and the subsequent isomerization and hydrogen abstraction reactions CH_2NO may undergo. These include the isomerization and subsequent dissociation reactions

$$CH_2NO(^2A') \rightarrow CH_2ON(^2A) \rightarrow CH_2(^3B_1) + NO(^2\Pi) \ , \quad (3)$$

the dissociation reaction

$$CH_2NO(^2A') \rightarrow HCNO(^1\Sigma) + H(^2S) \quad (4)$$

the abstraction reactions

$$HCNO(^1\Sigma) + H(^2S) \rightarrow CNO(^2\Sigma, ^2\Pi) + H_2(^1\Sigma_g) \quad (5)$$

and the molecular elimination reaction

$$CH_2NO(^2A') \rightarrow CNO(^2\Pi) + H_2(^1\Sigma_g) \ . \quad (6)$$

The purpose of this study is twofold. Firstly, our aim is to elucidate the thermally accessible, low-energy pathways by which these reactions may proceed by calculating accurate potential energy surfaces (PES) in the form of relative energies of the stationary points on the PES. The calculations have been performed using both the G2 approach and CASPT2 in conjunction with two different basis sets, namely Dunning's correlation-consistent polarized bases [28]: cc-pVDZ and cc-pVTZ. This enables us, secondly, to analyse and compare the performance of the above methods and to study both the methodological and basis set requirements associated with the reliable ab initio computation of PES in general and those of CH_2NO and HCNO in particular.

Accurate high-level ab initio computational studies, largely at CASSCF and MRCI levels, have already been carried out by Walch on several related systems, such as the reaction between N_2 and CH_2 [29], as well as between N_2 and CH [30], which resulted in useful information on the role of these reactions in the prompt NO mechanism.

2 Computational methods

Following the protocol of the G2 method [20] for molecules at equilibrium geometries, all stationary points on the PES of CH_2NO and of HCNO, including saddle points, were initially located at the SCF and MP2/6-31G(*d*) levels of theory (using the unrestricted formalisms UHF and UMP2 for open shell systems). The subsequent higher level and larger basis computations were carried out at the MP2/6-31G(*d*) geometries, while the zero-point vibrational energies (ZPE) were obtained at the UHF/6-31G(*d*) level and scaled by the recommended factor of 0.893. Both G2 and G2(MP2) methods aim at producing an energy that essentially reproduces the QCISD(T)/6-311 + G($3df$, $2p$) energy and further correct this by the addition of a small empirical quantity known as a higher level correction (HLC). The final G2 and G2(MP2) energies also include the (scaled) ZPE. Differences in the G2 energies between two species are therefore equivalent to differences in their heats and free energies of formation at 0 K. The G2 and G2(MP2) calculations were carried out using the Gaussian 94 system of programs [31].

The geometries and frequencies were also computed using the CASSCF method [16, 17], in conjunction with the cc-pVDZ basis sets of Dunning [28]. The frequencies were then scaled by 0.92 in accordance with a previous study (on pyrrole and its isomers) [32] where it was found that such a scaling yields ZPEs that are comparable with those employed by G2. Energies were obtained at the CASSCF and CASPT2 levels, using the cc-pVDZ as well as the larger cc-pVTZ basis. The CASSCF geometry optimizations were performed using the DALTON quantum chemistry program [33]. The CASPT2 calculations were carried out using the MOLCAS4 programs [34].

To ensure that reliable relative energies are obtained, the active space in the CASSCF and CASPT2 needs to be chosen with some care. A simple analysis suggests that the smallest active space that could correctly describe the formation of CH_2NO from CH_2 and

NO should consist of the π space of NO in addition to the open shell a_1 and b_1 orbitals of CH_2, i.e. a total of six orbitals accommodating seven active electrons. Unfortunately, such a space proved to be too small and gave rise to erratic results that strongly depended on the nature of the starting orbitals. Moreover, as the C–N bond in CH_2NO was stretched, the calculation failed to describe the dissociation correctly. It was subsequently found that in the course of the association reaction a high degree of interaction and mixing occurred between the in-plane π molecular orbitals and the lone pair (σ) orbitals of NO. Consequently, the number of active electrons was increased to 9 and then to 11, with a concomitant increase in the number of active orbitals. The latter would require a minimum of 8 active orbitals, but this was increased to 11, so as to provide an extra degree of flexibility and hence greater stability in the calculations. The results reported in this paper were all obtained using this final choice of 11 active electrons and 11 active orbitals, denoted 11/11. When calculating the energies of fragments the above choice of active space translates to 2/2 in CH_2, 9/9 in NO, 10/10 in HCNO and 11/11 in CNO.

Finally, so as to provide an additional basis for the evaluation of the performance of CASPT2, single-point QCISD(T) as well as coupled-cluster [CCSD(T) and RCCSD(T)] energy calculations were also carried out. In contrast with the QCI formalism, as implemented in the Gaussian 94 programs, the open shell coupled-cluster calculations use restricted Hartree-Fock (RHF) wave functions as reference states [35]. These latter calculations were performed using the MOLPRO programs [36]. All computations were carried out on DEC alpha 600/5/333 workstations.

It is pertinent to recall here that the development of the coupled-cluster methods, which have become one of the most important and accurate techniques of quantum chemistry, owe much to the pioneering work of Meyer [37, 38] who first formulated and applied the CEPA method to chemical problems. The relationship between coupled-cluster and the various coupled-pair theories, such as CEPA, has been discussed in detail by Ahlrichs and Scharf [39].

3 Results and discussion

The structures and computed geometric parameters obtained at the MP2/6-31G(*d*) and CASSCF(11/11)/cc-pVDZ levels of theory of the species that correspond to stationary points on the PES that have been studied in this work are summarized in Figs. 1–3. The G2 energies, CASPT2 electronic energies and the respective ZPEs of these species are given in Table 1.

In the case of equilibrium geometries the differences between the MP2 and CASSCF parameters are quite small and, as shown later, would hardly contribute to the differences in relative stabilities that were obtained by a range of computational techniques. However, in the case of transition state (TS) geometries in certain dissociation reactions, the differences are more significant, see e.g. TS3, TS5 and TS8. In the case of TS2, where a saddle point was located when using MP2, the CASSCF calculations failed to locate such a point. As discussed later in greater detail, a problem that we experienced with certain transition states is whether they can be regarded as real or an artefact of the computational method used, i.e. whether or not they are reproducible at all levels of theory, especially at higher levels.

The ground state geometry of CH_2NO (I1) is found to be planar at all levels of theory, the electronic state being $^2A'$. This is consistent with the conventional valence structure with four electrons in the π (a'') molecular orbitals (MO) delocalized over the three heavy atoms and the odd electron nominally occupying a $\sigma(a')$ MO localized on O. The lowest excited state is a

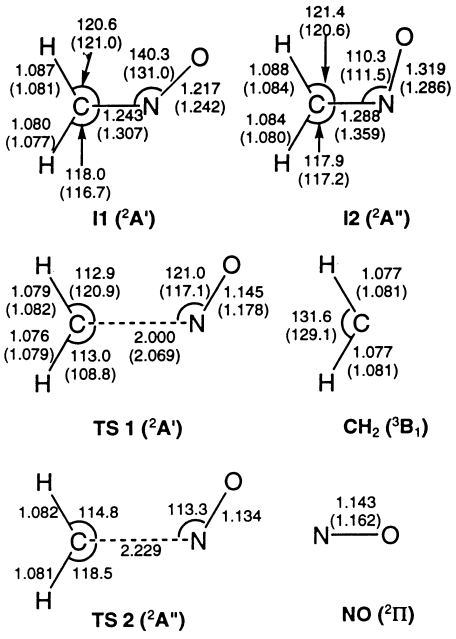

Fig. 1. MP2/6-31G(*d*) geometries and CASSCF(11/11)/cc-pVDZ geometries (in parentheses) of the species corresponding to stationary points on the potential energy surface (PES) describing the formation of CH_2NO (in Å and degrees)

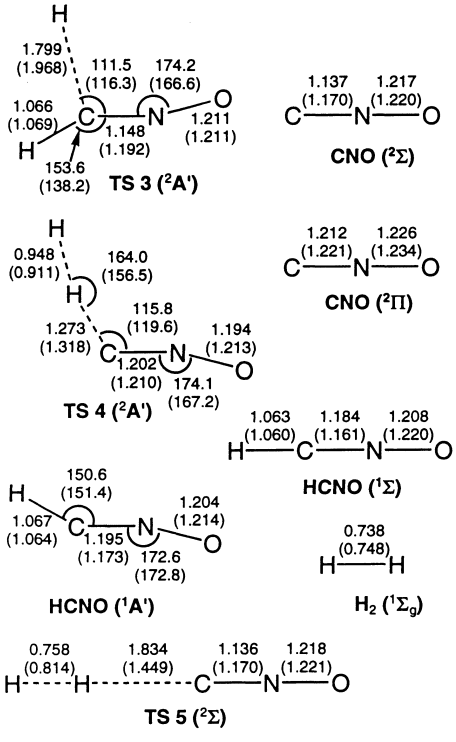

Fig. 2. MP2/6-31G(*d*) geometries and CASSCF(11/11)/cc-pVDZ geometries (in parentheses) of species corresponding to stationary points on the PES describing the loss and abstraction of hydrogen from CH_2NO (in Å and degrees)

$^2A''$ state (I2), with three electrons in the a'' MOs. A significant difference between the MP2 and CASSCF predictions is that the latter method does predict a

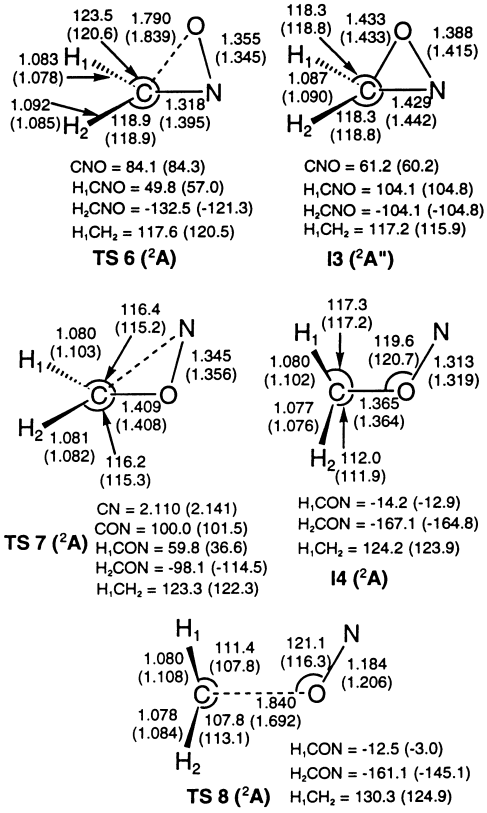

Fig. 3. MP2/6-31G(*d*) geometries and CASSCF(11/11)/cc-pVDZ geometries (in parentheses) of species corresponding to stationary points on the PES describing the isomerization and decomposition of CH_2NO (in Å and degrees)

planar equilibrium geometry, whereas the planar MP2 geometry gives rise to an imaginary a'' frequency, corresponding to an out-of-plane motion of one of the hydrogens, suggesting that at the MP2 level the equilibrium geometry is nonplanar.

The equilibrium structure of HCNO is found to be nonlinear by both MP2 and CASSCF methods, except for a CASSCF calculation with seven electrons in seven active orbitals which predicts a linear geometry. Given that the potential energy is very shallow, this is not surprising. The geometry of this molecule has been the subject of quite intensive study [40, 41], the final conclusion being that the molecule is slightly bent, with a barrier to linearity that is estimated to be just 2–6 cm^{-1}. For a given species, the SCF and CASSCF scaled ZPEs are generally within 1 kcal/mol of each other, indicating that the scaling factors used are reasonably consistent.

Geometry optimizations were also performed for a number of species at the CASSCF(9/9) level using the larger cc-pVTZ basis. The resulting changes in the geometries were found to be very small and the effects on the CASPT2/cc-pVTZ energies were similarly small, generally in the range 0.1–0.2 kcal/mol. Thus the use of the cc-pVDZ basis in CASSCF geometry optimizations appears justified.

3.1 PES of $CH_2 + NO \rightarrow CH_2NO$ reaction

The ground ($^2A'$) and first excited ($^2A''$) states of CH_2NO were studied. Both are formed by the interac-

Table 1. Total electronic and zero-point vibrational energies of reactants, products, intermediates and transition states associated with the formation, rearrangement and decomposition reactions of CH_2NO

	G2[a] (E_h)	ΔE_{ZPE}(G2) (kcal/mol)	CASPT2(11/11) cc-pVTZ (E_h)	ΔE_{ZPE}(CASSCF(11/11)) (kcal/mol)
CH_2NO ($^2A'$) (I1)	−168.930826	18.43	−168.928014	18.87
CH_2NO ($^2A''$) (I2)	−168.900925	18.16	−168.894037	18.54
TS1 ($^2A'$)	−168.808640	13.98	−168.797999	14.19
TS2 ($^2A''$)	−168.823604	14.35		
CH_2 ($^3B_1$)	−39.069016	10.32	−39.076558[b]	10.61[b]
NO ($^2\Pi$)	−129.739969	2.84	−129.722751[c]	2.54[c]
TS3 ($^2A'$)	−168.845751	11.71	−168.829232	12.39
TS4 ($^2A'$)	−168.822005	10.54	−168.805444	10.58
TS5 ($^2\Sigma$)	−168.787848	11.24	−168.782195	9.65
HCNO ($^1A'$)	−168.345058	12.88	−168.329700[d]	11.33[d]
HCNO ($^1\Sigma$)	−168.345292	12.88	−168.328571[d]	10.93[d]
H_2 ($^1\Sigma$)	−1.16636	5.93	−1.164568[e]	6.03[e]
CNO ($^2\Pi$)	−167.681385	5.28	−167.659958	4.97
CNO ($^2\Sigma$)	−167.621980	5.45	−167.607562	6.37
TS6 (^2A)	−168.865014	16.16	−168.860126	17.67
Cyclic CH_2NO ($^2A''$) (I3)	−168.907165	19.77	−168.900394	19.05
TS7 (^2A)	−168.829725	17.04	−168.829758	16.61
CH_2ON (^2A) (I4)	−168.841837	17.59	−168.843642	17.20
TS8 (^2A)	−168.782178	14.37	−168.799904	14.94

[a] G2 energy includes the zero-point correction ΔE_{ZPE}(G2)
[b] CASSCF(2/2)
[c] CASSCF(9/9)
[d] CASSCF(10/10)
[e] SCF

tion between methylene and NO in their respective ground states. A schematic PES, calculated at the G2 level, showing the formation of CH_2NO (as well as its subsequent decomposition to H + HCNO and then to H_2 and CNO) is shown in Fig. 4. The relative energies of the appropriate stationary points, calculated by a range of methods, are summarized in Table 2.

Concerning the formation of CH_2NO in C_s symmetry (corresponding to planar geometries) there are two distinct surfaces: A′ and A″, depending on the electronic configuration of NO in the reduced (C_s) symmetry (from $C_{\infty v}$), given that the electronic state of methylene is $^3A''$. On the A′ surface the electronic state of NO therefore needs to be $^2A''$, so its configuration is such that its out-of-plane π MOs contain three electrons, with two electrons in the in-plane π MOs. As the two fragments come together, the unpaired a'' electron on CH_2 couples with the unpaired a'' electron on NO in a straightforward π bond-forming interaction which, by itself, is expected to simply lower the energy. In addition, though, the singly occupied a' orbital on CH_2 interacts with the in-plane π MOs of NO, viz. both the doubly occupied and unoccupied (antibonding) a' MOs, resulting in three electrons in three-centre bonding and nonbonding MOs. According to the SCF calculations, however, the bonding MO is fairly strongly localised such that it effectively corresponds to a CN σ-bond, while the third electron resides predominantly on the oxygen, as implied by the valence structure discussed above. Consequently, a certain amount of electronic rearrangement takes place as the CN σ-bond forms, which may be expected to be associated with a small energy barrier. For the analogous situation on the A″ surface, NO starts off in the $^2A'$ state, i.e. with three electrons in the in-plane π (a') MOs and two electrons in the out-of-plane π (a'') MOs. As a result, the CN σ-bond can form without extensive electronic rearrangement, although some rearrangement is expected to take place among the π electrons as the CN π-bond forms. Thus, qualitatively, a smaller barrier may be anticipated than on the A′ surface.

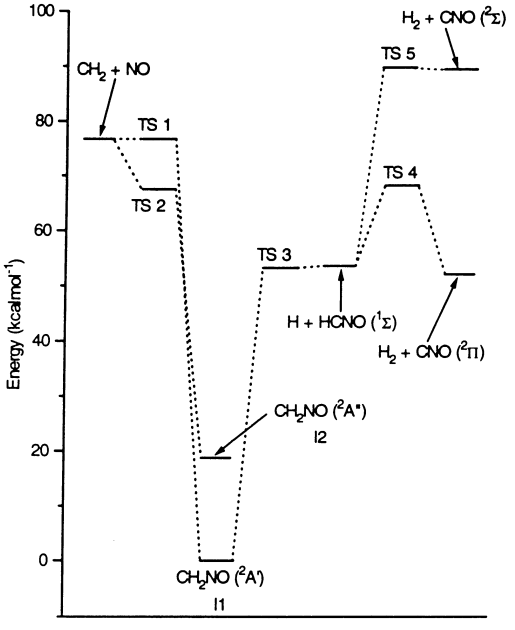

Fig. 4. Schematic G2 PES for the formation of CH_2NO and its decomposition to H + HCNO and H_2 + CNO

The above ideas appear to be borne out by the MP2 results. For example, the MP2/6-311G(*d,p*) barrier to association (TS2) is ~2.5 kcal/mol, considerably less than on the A′ surface, viz. ~19.6 kcal/mol (TS1). However, once the energies are recalculated at the QCI or G2 level, the energy of TS2 drops below the energy of the separated reactants by ~9 kcal/mol and the barrier disappears completely. It seems safe to conclude, therefore, that there is actually no barrier to association on the A″ surface. This is supported by the fact that no such transition state was found when using CASSCF. The saddle point TS1 on the A′ surface, on the other hand, has turned out to be a second order saddle point with an imaginary frequency for an a'' mode associated with an out-of-plane motion of the hydrogens, in addition to the imaginary frequency associated with the reaction coordinate. Moreover, at the G2 as well as the most extensive CASPT2 levels of theory, the barrier is so small that one may actually question its existence. In C_1 symmetry on the other hand, no saddle point was found in a series of CASSCF calculations. The most likely scenario is, therefore, that initially the association reaction proceeds on the A″ surface, or possibly on an A surface (with no symmetry), but at some point the system moves onto the

Table 2. Energies (including zero-point correction) of reactants $CH_2(^3B_1)$ + $NO(^2\Pi)$, saddle points and CH_2NO ($^2A''$) (relative to CH_2NO ($^2A'$), in kcal/mol)

	CH_2NO ($^2A''$) (I2)[a]	TS1 ($^2A'$)[b]	TS 2 ($^2A''$)	CH_2 ($^3B_1$) +NO($^2\Pi$) (P1)
MP2/6-311G(*d, p*)[c]	22.1	80.7	63.6	61.1
MP2/6-311 + G(3*df*, 2*p*)[c]	24.3	86.7	70.3	68.8
MP4/6-311G(*d, p*)[c]	18.8	76.0	62.0	60.9
QCISD(T)/6-311G(*d, p*)[c]	16.9	71.2	60.7	66.0
QCISD(T)/cc-pVTZ[c]	18.0	77.3	65.3	71.7
G2[c]	18.8	76.7	67.3	76.5
G2 (MP2)[c]	19.1	77.1	67.5	76.6
CASSCF(11/11)/cc-pVDZ[d]	13.7	66.4		48.7
CASPT2(11/11)/cc-pVDZ[d]	20.2	72.7		68.5
CASPT2(11/11)/cc-pVTZ[d]	21.0	76.9		75.0
RCCSD(T)/cc-pVTZ[d]	19.8	86.0		71.9
QCISD(T)/cc-pVTZ[d]	18.4	76.7		72.2

[a] First-order saddle point at MP2 level
[b] Second-order saddle point at both MP2 and CASSCF levels
[c] Computed at MP2/6-31G(*d*) geometries
[d] Computed at CASSCF(11/11)/cc-pVDZ geometries

A′ surface. The point of crossing between the A′ and A″ surfaces was found, with the help of MP2/6-31G(*d*) calculations, to occur at a CN distance of ~1.6 Å. The minimum energy path to the product CH_2NO in its $^2A'$ ground state is one where the system is planar ($^2A''$) in the region of CN distances of ~2.5 Å, becomes nonplanar at ~1.9 Å and then planar again ($^2A'$) at ~1.6 Å.

On comparing the dissociation energies of CH_2NO ($^2A'$) obtained, the agreement between the G2 and CASPT2 values appears to be quite good, although to some extent it is fortuitous. The G2 and G2(MP2) energies contain a HLC term of 2.9 kcal/mol as well as a fairly large correction for basis set incompleteness, 7.7 kcal/mol, of which the correlated calculations using the cc-pVTZ basis resolve ~5.7 kcal/mol. If full allowance was made for these corrections, the CASPT2 energy would become ~4.9 kcal/mol higher, resulting in a dissociation energy of ~80.0 kcal/mol. In our view the best correlated cc-pVTZ estimate of this energy is the QCISD(T) result of 71.7 or 72.2, depending on the choice of geometry. The QCI results were also found to be in close agreement (within 0.3 kcal/mol) with the corresponding RCCSD(T) values. For this reaction the G2 prediction of the dissociation energy is therefore expected to be accurate to within ~2 kcal/mol, in line with the accuracy of predicted atomization energies obtained by Curtiss et al. [20].

In the case of the energy difference between the $^2A''$ and $^2A'$ states of CH_2NO, the agreement between all the high-level correlated results is very good. In this case the basis set incompleteness effects are small and there are no HLC terms. However, there is a large discrepancy between the RCCSD(T) and QCISD(T) energies that were obtained for TS1. The reason for this is that at the TS1 geometry the RHF wave function of the molecule is inadequate as a reference state for a single-reference expansion of the correlated wave function. This is evident if the value of the T_1 diagnostic [42] is examined: this is very high (0.27) for this system, indicative of substantial near-degeneracy in the wave function. By comparison, $T_1 = 0.05$ for the ground state of CH_2NO (I1). The most direct evidence for near-degeneracy of course comes from the examination of the CASSCF wave function of TS1, which reveals that the two dominant configurations, $\ldots 9a'^2 10a'^1 1a''^2 2a''^2$ and $\ldots 9a'^2 10a'^1 1a''^2 3a''^2$, have coefficients of 0.77 and −0.45 respectively. Clearly, for a system such as TS1, the RCCSD(T) method is inapplicable. By contrast, the UHF based methods appear to perform quite well (in comparison with CASPT2) and appear to be free of near-degeneracy problems, although spin contamination in the UHF wave function is quite high ($\langle S^2 \rangle \approx 1.9$).

3.2 PES of $CH_2NO \rightarrow H + HCNO$ and $H + HCNO \rightarrow H_2 + CNO$ reactions

The salient features of the PES for these reactions are shown in Fig. 4. The relative energies are given in Table 3. Loss of a hydrogen atom from CH_2NO (I1) takes place on the $^2A'$ surface and proceeds via TS3 to yield H + HCNO (fulminic acid) (P2 or P3). At the MP2 and MP4 levels TS3 (with one imaginary frequency) is of higher energy than the dissociated products, but at the QCI and G2 levels TS3 is approximately isoenergetic with the products, or even lower in energy. The CASPT2 calculations produced quite similar results. Therefore, this transition state may well not exist (in analogy with the situation for TS2), despite the considerable electronic rearrangement that is expected to occur as HCNO forms, either as a linear ($^1\Sigma$) or bent ($^1A'$) molecule. Evidently, the effects of such a rearrangement, in the form of a barrier, are obvious at MP2, MP4 and CASSCF (and SCF) levels of theory, but not at a highly correlated level. The minimum in the MP2 PES of HCNO corresponds to a bent configuration in which the hydrogen is *trans* to the oxygen (P2); there appears to be no minimum corresponding to a *cis* configuration. If it is the hydrogen *trans* to the oxygen in CH_2NO that is being removed, we find that the oxygen flips around to the other side so that the

Table 3. Energies (including zero-point correction) of products and transition states associated with the decomposition of CH_2NO to H + HCNO and H_2 + CNO (relative to CH_2NO ($^2A'$), in kcal/mol)

	TS3 ($^2A'$)	H + HCNO ($^1A'$) (P2)	H + HCNO ($^1\Sigma$)[a] (P3)	TS4 ($^2A'$)	TS5 ($^2\Sigma$)[b]	H_2 + CNO ($^2\Pi$) (P4)	H_2 + CNO ($^2\Sigma$) (P5)
MP2/6-311G(*d*, *p*)[c]	52.1	33.8	34.4	69.7	94.5	48.9	93.0
MP2/6-311 + G(3*df*, 2*p*)[c]	51.0	34.0	34.2	70.1	94.3	52.7	93.7
MP4/6-311G(*d*, *p*)[c]	53.3	39.4	40.4	68.3	93.9	45.7	92.8
QCISD(T)/6-311G(*d*, *p*)[c]	54.3	52.8	53.0	67.6	90.0	48.0	88.6
QCISD(T)/cc-pVTZ[c]	54.0	54.4	54.5	68.4	91.9	51.3	90.3
G2[c]	53.4	53.8	53.7	68.3	89.7	52.1	89.4
G2 (MP2)[c]	53.3	53.0	53.0	68.0	89.7	51.8	89.3
CASSCF(11/11)/cc-pVDZ[d]	55.5	49.0	49.0	81.2	92.4	38.8	82.6
CASPT2(11/11)/cc-pVDZ[d]	55.2	54.3	55.2	67.9	83.6	54.0	90.6
CASPT2(11/11)/cc-pVTZ[d]	55.5	54.2	54.5	68.6	82.3	57.1	91.3
RCCSD(T)/cc-pVTZ[d]	54.8	53.0	52.7	73.4	81.9	52.4	90.5
QCISD(T)/cc-pVTZ[d]	54.7	53.3	53.0	68.7	82.3	51.8	90.6

[a] Second-order saddle point at MP2 and CASSCF levels
[b] Third-order saddle point at CASSCF level
[c] Computed at MP2/6-31G(*d*) geometries
[d] Computed at CASSCF(11/11)/cc-pVDZ geometries

leaving hydrogen is once again *cis* to the oxygen, resulting in the same transition state for dissociation, i.e. TS3, and resulting in *trans* HCNO as the product. Our calculations indicate that whilst at the MP2 level linear HCNO ($^1\Sigma$) (P3) is marginally higher in energy than the bent form (the barrier to linearity being ~ 0.6 kcal/mol), its G2 energy is marginally lower (by about 0.15 kcal/mol). Given the extremely flat bending potential of HCNO, as demonstrated by several high-level calculations, the above results are rather characteristic of what one encounters when studying this molecule.

Once the first hydrogen has been lost the second may be removed by direct dissociation or abstraction. The first alternative yields, as overall products, $2H + CNO$, which lie very high energetically and will not be considered further. Abstraction of H by another H atom to form $H_2 + CNO$ (P4 or P5) is a much more favourable process that could proceed either by side-on or by end-on attack by H. The difference in the barrier to abstraction between the two processes is around 21 kcal/mol, with side-on attack being the lower energy option. The rationale behind this is that side-on attack produces CNO in its $^2\Pi$ ground state whereas end-on attack produces the $^2\Sigma$ first excited state. In the case of TS5, all calculations at the MP2/6-31G(*d*) geometry, including G2, predict it to be slightly higher in energy than the products, i.e. the reverse process is predicted to have a small barrier to recombination. The CASPT2 results are qualitatively different from the above, in that TS5 is energetically ~ 9 kcal/mol below the products. The reason for this large, qualitative difference is due to the large differences between the MP2 and CASSCF geometries of TS5, as remarked earlier. The CASSCF geometry is much tighter than its MP2 counterpart, with an almost 0.4 Å difference in the respective H–C distances. Moreover, the CASSCF geometry for TS5 also represents a higher-order saddle point, with imaginary bend frequencies, in addition to the σ-mode representing the reaction coordinate. Thus, on the basis of these latter results the existence of a proper transition state is doubtful.

With regard to the stability of the CNO radical, there are noticeable differences between the CASPT2 and the G2 results, in particular in the case of the $^2\Pi$ state, where the CASPT2 energy lies fully 5 kcal/mol above the G2 value. Given that this system is a molecule at its equilibrium geometry, not a transition state with an unusual geometry, G2 is expected to reproduce its relative energies to within ~ 2 kcal/mol. The close agreement between the G2 and QCISD(T) [as well as CCSD(T)] results obtained using the cc-pVTZ basis, irrespective of geometry, suggests that the discrepancy is not due to deficiencies in the cc-pVTZ basis but rather a (small) deficiency in the perturbational estimate of dynamical correlation effects that is implicit in the CASPT2 method. In this instance, however, a useful comparison with experiment can also be made, since the $X^2\Pi \rightarrow {}^2\Sigma$ excitation energy has been measured [43] as 36.0 kcal/mol. Our calculated G2 and CASPT2 values actually bracket the experimental value, as they are 37.3 and 34.2 kcal/mol respectively. The CASPT2 result is in good agreement with the result of Persson et al. [44], viz. 33.8 kcal/mol, also obtained by CASPT2 in a (14,9,4,3)/[4,3,2,1] atomic natural orbital basis set. Thus, at least as far as the excitation energy is concerned, we cannot decide in favour of one approach or the other.

CH_2NO may undergo loss of H_2 by the sequential hydrogen loss/hydrogen abstraction process described above. Such a bimolecular reaction though is unlikely to occur in a combustion process, since it requires fairly high concentrations of H and HCNO. A more likely option may be expected to be the concerted loss, viz. molecular elimination of H_2, as occurs, for example, in formaldehyde [45, 46] and ethylene [47]. However, we were unable to locate a transition state for this process. The searches yielded either TS4 or TS5. From this we may conclude that the energy barrier for concerted loss of H_2, if it exists, is at least that of TS4 (that is, 68.3 kcal/mol, as given by G2). We note also that the energetics of the two decomposition reactions, giving $H + HCNO$ and $H_2 + CNO$ respectively as products, are nearly the same. If we make a conservative estimate of the reverse barrier height associated with hypothetical H_2 elimination from CH_2NO as ~ 5 kcal/mol, the loss of H will be clearly the energetically preferred channel. On the ground state PES the search for the lowest energy saddle point is then likely to lead to the product region, i.e. $H + HCNO$ (where the curvature with respect to the reaction coordinate is of course negative). By contrast, in formaldehyde the barrier height associated with H_2 elimination is ~ 5 kcal/mol below the energy of dissociation to $H + HCO$, as calculated from the data of Scuseria and Schaefer [48] and Yates et al. [49]. In ethylene the corresponding energy difference is ~ 16 kcal/mol, based on the calculations of Jensen et al. [47] and Ochterski et al. [50].

In the case of TS4, the RCCSD(T) and QCISD(T) results differ by 4.7 kcal/mol, which is a considerably larger discrepancy than has been generally found for any of the other species studied in this work, with the exception of TS1, which was demonstrated to be ill-suited for a RCCSD(T) study. The situation is less clear-cut, however, in the case of TS4. The value of the T_1 diagnostic is 0.10, which suggests a reasonably high degree of near-degeneracy. On the other hand, the dominant configuration in the CASSCF wave function, which is a single determinant, has a coefficient of ~ 0.93, which is comparable with what has been observed for most other transition states.

3.3 PES of $CH_2NO \rightarrow CH_2ON$ isomerization and subsequent decomposition

The PES for the isomerization of CH_2NO to CH_2ON and the subsequent decomposition of the latter are shown in Fig. 5. The corresponding energies are given in Table 4. The sequence of reactions discussed here proceeds via a cyclization reaction to the cyclic intermediate (I3) that is relatively stable, followed by a ring opening reaction yielding CH_2ON (I4) which can then decompose to methylene and nitric oxide. The first step is the breaking of the C_s symmetry of CH_2NO: as the CNO angle decreases and the carbon-oxygen bond forms, the two hydrogens twist out of the plane. The barrier height to this cyclization leading to the saddle

point TS6 is 41.3 kcal/mol at the G2 level. The cyclic isomer of CH_2NO (I3) that forms has C_s symmetry again; its ground state is $^2A''$ and lies just 14.8 kcal/mol above CH_2NO ($^2A'$) according to the G2 calculations. It has a surprisingly low energy in light of the highly strained ring system. This may be attributed to the presence of a partial π-bond between the N and O atoms, i.e. three electrons occupying the (bonding and antibonding) $1a''$ and $3a''$ MOs. Further stabilization is possible by hyperconjugation, e.g. stabilizing interactions between the $4a''$ C–H (unoccupied antibonding) MO and the $1a''$ MO.

Rupture of the CN bond, resulting in CH_2ON (I4) via TS7 involves a further barrier of 48.6 kcal/mol, as predicted by G2. CH_2ON is a nonplanar molecule and its relative instability is typical of compounds with CON groups. The π-bonding in this group is very weak: the four π electrons reside in a weakly bonding π MO that effectively accommodates a lone pair on O, while the remaining electrons from C and N occupy a nonbonding MO. The Lewis structure describing this situation effectively consists of only two σ-bonds connecting the heavy atoms, with only oxygen having its full complement of two bonds. The relative weakness of the NO bond in I4 is of course manifested in its length, 1.313 Å, to be compared with the NO distances in nitric oxide and CH_2NO, viz. 1.143 Å and 1.217 Å respectively.

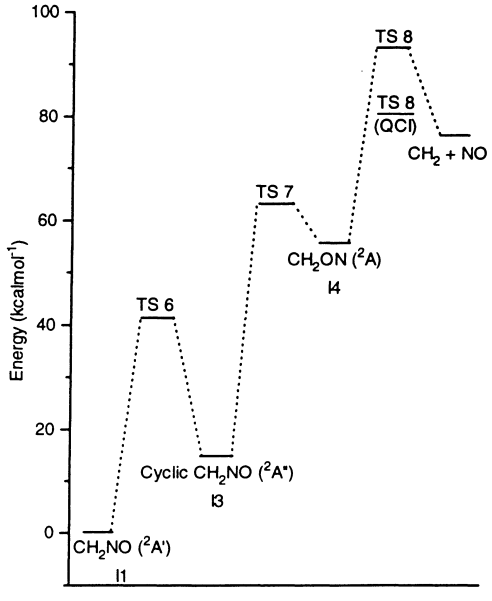

Fig. 5. Schematic G2 PES for the isomerization of CH_2NO to CH_2ON and dissociation. (The QCI energy for TS8 is the QCISD(T)/cc-pVTZ//CASSCF(11/11)/cc-pVDZ value)

Breaking the CO bond in CH_2ON regenerates the original reactants: methylene and nitric oxide. The G2 barrier height of 37.4 kcal/mol (at TS8) is judged rather high for such a dissociation, considering the low endothermicity of this reaction: 20.6 kcal/mol at the G2 level. The CASPT2/cc-pVTZ calculations predict a considerably lower barrier of 25.2 kcal/mol and an endothermicity of 23.8 kcal/mol. With respect to the barrier height we believe the CASPT2 results to be more reliable. Most of the difference between the G2 and CASPT2 results can be traced to the large differences in the geometries used, i.e. those computed at the MP2/6-31G(*d*) and CASSCF(11/11)/cc-pVDZ levels respectively, which are most significant for the C–O distance. As in the case of TS5, we believe the CASSCF geometry to be the more accurate one. The analogous QCISD(T)/cc-pVTZ calculations of the barrier height and endothermicity yield 26.0 kcal/mol and 17.7 kcal/mol respectively when computed at the CASSCF geometries. This suggests that our CASPT2 calculations overestimate the heat of this reaction. The above results also indicate that the reaction of CH_2 with NO to produce CH_2ON has a relatively low barrier: just 1.4 kcal/mol when computed using CASPT2, 8.3 kcal/mol when using QCISD(T)/cc-pVTZ, both at the CASSCF geometries, or 16.8 kcal/mol at the G2 level, noting that the last value is expected to be an overestimate by $\sim$10 kcal/mol.

Comparing the G2, CASPT2 and QCISD(T) results at the other stationary points on this PES, we note that the agreement is quite similar to what has been observed before, i.e. the CASPT2 predictions differ from the rest by up to $\sim$ 5 kcal/mol. On comparing the RCCSD(T) and QCISD(T) results we note that their respective predictions differ most when applied to transition states, although for the current series, viz. TS6, TS7 and TS8, the RCCSD(T) barriers are lower than those obtained by QCISD(T). This is the opposite of what has been

Table 4. Energies (including zero-point correction) of isomers and transition states associated with the rearrangement of CH_2NO to CH_2ON and subsequent decomposition to $CH_2(^3B_1) + NO(^2\Pi)$ (relative to CH_2NO ($^2A'$), in kcal/mol)

	TS6 (^{2}A)	Cyclic CH_2NO ($^2A''$) (I3)	TS7 (^{2}A)	CH_2ON (^{2}A) (I4)	TS8 (^{2}A)
MP2/6-311G(*d*, *p*)[a]	54.5	9.1	60.2	53.5	97.8
MP2/6-311+G(3*df*, 2*p*)[a]	55.6	9.5	64.6	57.7	103.3
MP4/6-311G(*d*, *p*)[a]	50.1	9.6	58.6	51.9	92.7
QCISD(T)/6-311G(*d*, *p*)[a]	40.6	14.1	59.3	51.8	88.3
QCISD(T)/cc-pVTZ[a]	40.5	14.4	61.3	54.0	87.4
G2[a]	41.3	14.8	63.4	55.8	93.3
G2 (MP2)[a]	41.7	14.6	63.6	56.0	93.9
CASSCF(11/11)/cc-pVDZ[b]	43.2	22.7	59.0	53.7	82.1
CASPT2(11/11)/cc-pVDZ[b]	41.9	18.8	57.3	49.3	73.1
CASPT2(11/11)/cc-pVTZ[b]	41.4	17.5	59.4	51.3	76.5
RCCSD(T)/cc-pVTZ[b]	39.5	14.4	60.7	53.5	78.0
QCISD(T)/cc-pVTZ[b]	42.6	14.5	61.7	54.5	80.5

[a] Computed at MP2/6-31G(*d*) geometries
[b] Computed at CASSCF(11/11)/cc-pVDZ geometries

found for TS1 and TS4. Given that for the current series the evidence for the applicability of the RCCSD(T) method is more convincing, such as lower values of T_1 ($\sim$0.06), it seems plausible that for these systems the RCCSD(T) results are more accurate than those from the QCISD(T) calculations, especially in view of the spin contamination in the UHF reference states and hence QCI wave functions.

3.4 Comparison of computational methods

Inspection of the computed energies of the various species that correspond to stationary points on the PES studied as summarized in Tables 2–4 allows some general statements considering the performance of the various computational techniques used to be made. With regard to molecular energies, the MP2 method is generally quite inadequate, especially in the prediction of dissociation energies and barrier heights. This is hardly unexpected. MP4 represents a significant improvement, but when compared with QCISD(T) it is clear that MP4 estimates of dissociation energies could be in error by over 10 kcal/mol, e.g. in the case of reaction (4). The G2 and G2(MP2) energies, as expected, are uniformly very close, the maximum difference being less than 1 kcal/mol. Comparing the QCISD(T)/cc-pVTZ and G2 energies we note that, with the exception of TS8, there is good agreement among the two sets of results, especially in the case of equilibrium geometries, provided that allowance is made for the presence of the HLC term in G2. This may be taken as a demonstration of the capability and adequacy of the cc-pVTZ basis for calculations of the type undertaken in this work, but also as a verification of the adequacy of lower level, such as MP2, estimation of basis set incompleteness that is implicit in the G2 and G2(MP2) treatments.

When comparing the CASSCF and CASPT2 results with G2, the possible effects that result from the different geometries used must be considered. In the case of equilibrium geometries this effect is small, as demonstrated by the close agreement between the QCI energies that were obtained using the same basis at the respective CASSCF/cc-pVDZ and MP2/6-31G(*d*) geometries. However, for transition states, where the applicability of the MP2 method for geometry optimization may be questioned, the differences are expected to be larger. As discussed in Sects. 3.2 and 3.3, in the case of TS5 and TS8 the MP2 and CASSCF geometries differ significantly, resulting in fairly large differences in the predicted energies. This significantly reduces the barrier height to decomposition via TS8 and actually eliminates it in the case of TS5. Moreover, at these geometries there is some indication that the validity of estimating the effects of basis set incompleteness at the MP2 and MP4 levels is doubtful. For example, in the case of TS8 the QCI energies obtained using the cc-pVTZ and 6-31G(*d*) bases (at the MP2 geometry) differ by −0.9 kcal/mol, whereas the difference between the MP2/6-311+G(3df,2p) and MP2/6-31G(*d*) energies is 5.5 kcal/mol. This results in a difference of 5.9 kcal/mol between the G2 and QCISD(T)/cc-pVTZ energies.

Comparison of CASPT2 and QCISD(T) energies (at the CASSCF geometries) indicates that the level of agreement is mostly reasonably good, the mean and maximum deviations being 1.9 and 5.3 kcal/mol respectively. Nevertheless, in the case of transition states, where the possibility of substantial near-degeneracy exists, we would favour the CASPT2 results. The CASSCF energies show much larger fluctuations when compared with CASPT2 or QCI, indicating that in many situations that arise in studies of PES, such as the calculation of dissociation energies, dynamical correlation cannot be neglected. The plots in Fig. 6, displaying the differences between G2, CASPT2 and QCISD(T) energies at each stationary point on the PES of the CH_2NO molecule, illustrate graphically the level of consistency and agreement between the different techniques used in this study.

For most systems RCCSD(T) and QCISD(T) calculations, when carried out at the same geometry and using the same basis set, yield reaction energies and barrier heights that agree to within 1–2 kcal/mol. As discussed in Sects. 3.1 and 3.2, a reasonable level of care needs to be exercised when applying the RCCSD(T) method, since in situations where a substantial degree of near-degeneracy is present, a RHF-based expansion of the wave function is likely to yield unreliable results. In this respect, the T_1 diagnostic plays an important and valuable role. On the other hand, when the RCCSD(T) formalism is demonstrably applicable, as in Sect. 3.3, it is expected to be more reliable than the spin-unrestricted QCI method. In these situations the RCCSD(T) technique is therefore a viable alternative to CASPT2. Although in the majority of the calculations reported in this paper T_1 has been found to be substantially higher than the recommended "safe" value [42] of 0.02, we believe that the coupled-cluster method is probably

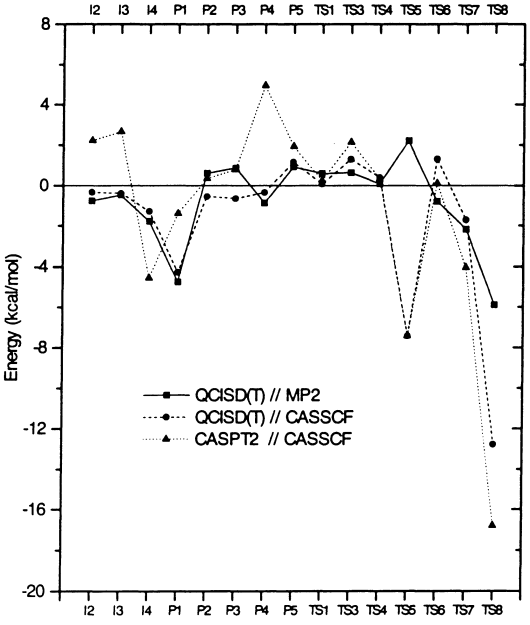

Fig. 6. Comparison of G2, QCISD(T)/cc-pVTZ//MP2/6-31G(d), QCISD(T)/cc-pVTZ//CASSCF(11/11)/cc-pVDZ and CASPT2(11/11)/cc-pVTZ//CASSCF(11/11)/cc-pVDZ energies, displayed as deviations from G2

sufficiently robust to cope with a higher level of near-degeneracy than implied by the above recommendation.

4 Conclusion

The quantum chemical study reported in this paper has explored some aspects of the reaction between methylene and NO, namely the formation of CH_2NO and some of the subsequent isomerization and dissociation reactions that can occur. At high temperatures both isomers, CH_2NO and CH_2ON, could form and interconvert by a unimolecular process. CH_2NO ($^2A'$) is found to be the most stable isomer, and it is predicted to form by a barrierless combination of CH_2 and NO. Other reactions that are expected to occur are the decomposition to $HCNO + H$ and, at least on energetic grounds, the abstraction reaction resulting in $H_2 + CNO$. No molecular elimination channel leading to $H_2 + CNO$ was found.

The reaction energies, as predicted by G2, are expected to be accurate to within $\sim$2 kcal/mol, but larger uncertainties are anticipated in the computed barrier heights associated with transition states. For these, in the absence of MRCI data, CASPT2 is judged to be the most reliable method, or a coupled-cluster treatment, such as QCISD(T) or RCCSD(T), carried out at CASSCF geometries with an appropriate basis, such as cc-pVTZ.

Acknowledgement. The award of a Sydney University Postgraduate Scholarship to W.A.S. is gratefully acknowledged.

References

1. Miller JA, Bowman CT (1989) Prog Energy Combust Sci 15:287 and references therein
2. Fenimore CP (1971). In: 13th Symposium (International) on Combustion. The Combustion Institute, Pittsburgh, p 373
3. Wendt JOL, Sternling CV, Matovich MA (1973). In: 14th Symposium (International) on Combustion. The Combustion Institute, Pittsburgh, p 897
4. Myerson AL (1975). In: 15th Symposium (International) on Combustion. The Combustion Institute, Pittsburgh, p 1085
5. Song YH, Blair DW, Siminski VJ, Bartok W (1981). In: 18th Symposium (International) on Combustion. The Combustion Institute, Pittsburgh, p 53
6. Chen SL, McCarthy JM, Clark WD, Heap MP, Seeker WR, Pershing DW (1986). In: 21st Symposium (International) on Combustion. The Combustion Institute, Pittsburgh, p 1159
7. Laufer AH, Bass AM (1974) J Phys Chem 78:1344
8. Vinckier C, Debruyn W (1979) J Phys Chem 83:2057
9. Seidler V, Temps F, Wagner HGG, Wolf M (1989) J Phys Chem 93:1070
10. Atakan B, Kocis D, Wolfrum J, Nelson P (1992). In: 24th Symposium (International) on Combustion. The Combustion Institute, Pittsburgh, p 691
11. Cyr DR, Leahy DJ, Osborn DL, Continetti RE, Neumark DM (1993) J Chem Phys 99:8751
12. Farmer JB, Gardner CL, Gerry MCL, McDowell CA, Raghunathan P (1971) J Phys Chem 75:2448
13. McCluskey M, Frei H (1993) J Phys Chem 97:5204
14. Wahl AC, Das G (1977). In: Schaefer HF (ed) Methods of electronic structure theory. Plenum, New York, p 51
15. Werner H-J, Meyer W (1980) J Chem Phys 73:2342
16. Roos BO, Taylor PR, Siegbahn PES (1980) Chem Phys 48:157
17. Roos BO (1987). In: Lawley KP (ed) Ab initio methods in quantum chemistry II. Wiley, Chichester, p 399
18. Pople JA, Head-Gordon M, Fox DJ, Raghavachari K, Curtiss LA (1989) J Chem Phys 90:5622
19. Curtiss LA, Jones C, Trucks GW, Raghavachari K, Pople JA (1990) J Chem Phys 93:5622
20. Curtiss LA, Raghavachari K, Trucks GW, Pople JA (1991) J Chem Phys 94:7221
21. Curtiss LA, Raghavachari K, Pople JA (1993) J Chem Phys 98:1293
22. Pople JA, Head-Gordon M, Raghavachari K (1987) J Chem Phys 87: 5968
23. Werner H-J (1987). In: Lawley KP (ed) Ab initio methods in quantum chemistry II. Wiley, Chichester, p 1
24. Andersson K, Malmqvist P-Å, Roos BO, Sadlej AJ, Wolinski K (1990) J Phys Chem 94:5483
25. Andersson K, Malmqvist P-Å, Roos BO (1992) J Chem Phys 96:1218
26. Fülscher MP, Andersson K, Roos, BO (1992) J Phys Chem 96:9204
27. Andersson K, Roos, BO (1993) Int J Quantum Chem 45:591
28. Dunning TH (1989) J Chem Phys 90:1007
29. Walch SP (1995) J Chem Phys 103:4930
30. Walch SP (1993) Chem Phys Lett 208:214
31. Frisch MJ, Trucks GW, Schlegel HB, Gill PMW, Johnson BG, Robb MA, Cheeseman JR, Keith T, Petersson GA, Montgomery JA, Raghavachari K, Al-Laham MA, Zakrzewski VG, Ortiz JV, Foresman JB, Peng CY, Ayala PY, Chen W, Wong MW, Andres JL, Replogle ES, Gomperts R, Martin RL, Fox DJ, Binkley JS, Defrees DJ, Baker J, Stewart JP, Head-Gordon M, Gonzalez C, Pople JA (1995) Gaussian 94, revision B.3. Gaussian, Pittsburgh, Pa
32. Bacskay GB, Martoprawiro M, Mackie JC (1998) Chem Phys Lett 290:391
33. Helgaker T, Jensen HJAa, Jørgensen P, Olsen J, Ruud K, Ågren H, Andersen T, Bak KL, Bakken V, Christiansen O, Dahle P, Dalskov EK, Enevoldsen T, Fernandez B, Heiberg H, Hettema H, Jonsson D, Kirpekar S, Kobayashi R, Koch H, Mikkelsen KV, Norman P, Packer MJ, Saue T, Taylor PR, Vahtras O (1997) DALTON, an ab initio electronic structure program, release 1.0
34. Andersson K, Blomberg MRA, Fülscher MP, Karlström G, Lindh R, Malmqvist P, Neogrády P, Olsen J, Roos BO, Sadlej AJ, Schütz M, Seijo L, Serrano-Andrés L, Siegbahn PEM, Widmark P-O (1997) MOLCAS, version 4. Lund University, Sweden
35. Knowles PJ, Hampel C, Werner H-J (1993) J Chem Phys 99:5219
36. Werner H-J, Knowles PJ, Almlöf J, Amos RD, Deegan MJO, Elbert ST, Hampel C, Meyer W, Peterson K, Pitzer R, Stone AJ, Taylor PR, Lindh R, Mura ME, Thorsteinsson T (1997) MOLPRO, version 97.4. University of Birmingham, UK
37. Meyer W (1971) Int J Quantum Chem Symp 5:341
38. Meyer W (1973) J Chem Phys 58:1017
39. Ahlrichs R, Scharf P (1987). In: Lawley KP (ed) Ab initio methods in quantum chemistry I, Wiley, Chichester, p 501
40. Rendell AP, Lee TJ, Lindh R (1992) Chem Phys Lett 194:84
41. Koput J, Winnewisser BP, Winnewisser M (1996) Chem Phys Lett 255:357
42. Lee TJ, Taylor PR (1989) Int J Quantum Chem Symp 23:199
43. Ramsay DA, Winnewisser M (1983) Chem Phys Lett 96:502
44. Persson BJ, Roos BO, Simonson M (1995) Chem Phys Lett 234:382
45. Minyaev RM, Wales DJ (1994) J Chem Soc Faraday Trans 90:1839
46. Chen W, Hase WL, Schlegel HB (1994) Chem Phys Lett 228:436
47. Jensen JH, Morokuma K, Gordon MS (1994) J Chem Phys 100:1981
48. Scuseria GE, Schaefer HF (1989) J Chem Phys 90:3629
49. Yates BF, Yamaguchi Y, Schaefer HF (1990) J Chem Phys 93:8798
50. Ochterski JOW, Petersson GA, Wiberg KB (1995) J Am Chem Soc 117:11299